Semiconductors, Vol. 39, No. 10, 2005, pp. 1224–1228. Translated from Fizika i Tekhnika Poluprovodnikov, Vol. 39, No. 10, 2005, pp. 1266–1270.

PHYSICS OF SEMICONDUCTOR DEVICES

Structural Mechanisms of Optimization of the Photoelectric Properties of CdS/CdTe Thin-Film Heterostructures

G. S. Khrypunov

Kharkov Polytechnical Institute (National Technical University), Kharkov, 61002 Ukraine

e-mail: khrip@ukr.net

Submitted January 24, 2005; accepted for publication February 3, 2005

Abstract—Comparative studies of the effect of chloride treatment of CdS/CdTe thin-film heterostructures on the output characteristics of ITO/CdS/CdTe/Cu/Au solar cells and the crystal structure of their base CdTe layer are carried out. Structural mechanisms determining variation in the efficiency of photoelectric processes in ITO/CdS/CdTe/Cu/Au thin-film solar cells produced by varying the thickness of the $CdCl_2$ layer during the chloride treatment are suggested. It is shown for the first time by X-ray diffractometry that the metastable hexagonal CdTe phase transforms into a stable cubic modification during the chloride treatment. This circumstance provides a substantial improvement in the photoelectric properties of CdS/CdTe thin-film heterostructures.

1. INTRODUCTION

The potential to solve energy-related environmental problems lies in the wide-scale use of environmentally clean ground-based renewable energy sources, specifically, photoelectric converters of solar radiation [1]. Currently, the efficiency of the best laboratory samples of CdS/CdTe thin-film solar cells approaches the efficiency of conventional solar cells based on single-crystal Si [2]. However, thin-film solar cells are more economical due to their low material and energy cost [3].

From the point of view of solid-state physics, CdS/CdTe-based solar cells are new objects, specifically, multilayer polycrystalline thin-film heterostructures. Due to the developed grain-boundary surface of the base CdTe layer and the high temperatures required to obtain such device structures, phase interaction significantly affects the solar cell efficiency [3]. Chloride treatment is an obligatory technological operation in the fabrication of high-efficiency CdS/CdTe-based thin-film solar cells [2]. This treatment increases the solar cell efficiency by a factor of 5–6 due to the phase interaction of the base layer with $CdCl_2$ [2]. One of the main causes of an increase in solar cell efficiency is an increase in the minority-carrier lifetime [4]. This increase is usually attributed to the experimentally identified decrease in the degree of development and inhibition of the grain-boundary surface of the CdTe layer [5, 6]. However, the structural variations inside the grains have not been analyzed in sufficient detail. This circumstance has impeded further optimization of the design and technology for CdS/CdTe-based thin-film solar cells [2]. Thus, study of the structural mechanisms of optimization of the photoelectric properties of CdS/CdTe thin-film heterostructures during chloride treatment solves a concrete applied problem. At the same time, such studies are of interest for physical materials science of a new class of solid objects.

2. EXPERIMENTAL

In order to obtain laboratory samples of ITO/CdS/CdTe/Cu/Au solar cells, 0.4-μm-thick CdS films were deposited by thermal evaporation at 200°C on glass substrates with a preliminarily deposited 0.5-μm-thick ITO (indium–tin oxide) layer. Then, 4-μm-thick CdTe films were deposited without a vacuum break at a substrate temperature of 300°C. After that, the chloride treatment of the base layers was carried out. For this purpose, $CdCl_2$ films were deposited by thermal evaporation in a vacuum chamber on the surface of the CdTe layer without heating the substrate. The obtained ITO/CdS/CdTe/$CdCl_2$ heterostructures were thermally treated in air in a closed volume at 430°C for 25 min. Then, the annealed heterostructures were etched in a bromomethanol solution to remove the by-products of the phase interaction, and two-layer Cu–Au contacts were formed by thermal evaporation on the CdTe surface.

The efficiency (η) and output parameters of the solar cells, specifically, the open-circuit voltage U_{oc}, the density of the short-circuit current I_{sc}, and the filling factor (FF) of the current–voltage (I–V) characteristics under illumination, were determined from the I–V characteristic under illumination at a luminous flux density of 100 W/cm^2.

In order to reveal the specific structural features of the CdTe base layers prior to and after the chloride treatment, we used the following complex of procedures for detecting and recording the diffraction spectra [7, 8]:

(i) The diffraction spectrum was automatically recorded under continuous 2θ scanning in the angle range 2θ = 20°–120° using Bragg–Brentano focusing of radiation from a copper anode. During such recording, the diffraction pattern is formed by the grains with reflection planes [*hkl*] parallel to the sample surface.

(ii) The diffraction reflections from the planes of the sphalerite and wurtzite modifications of CdTe, which are not revealed by the above detection method due to the fact that such samples are textured, were detected and point-by-point recorded in radiation from an iron anode by the method of θ/2θ scanning according to the procedure of so-called skew recording. For this purpose, a sample was rotated relative to its initial position by the corresponding angle between the plane that formed the most intense diffraction peak under the Bragg–Brentano focusing and the specified plane. The use of softer X-ray radiation allowed us to increase the angle spacing between the diffraction peaks.

(iii) The point-by-point recording of the profiles of the diffraction peaks was carried out by the method of ω scanning in order to determine the degree of texture scattering, which is expressed in terms of the half-width of the diffraction profile (in arc degrees) in the ω curve.

The precise determination of the lattice period was carried out using the extrapolation function $(\cos^2\theta/\sin\theta) + (\cos^2\theta/\theta)$ [9].

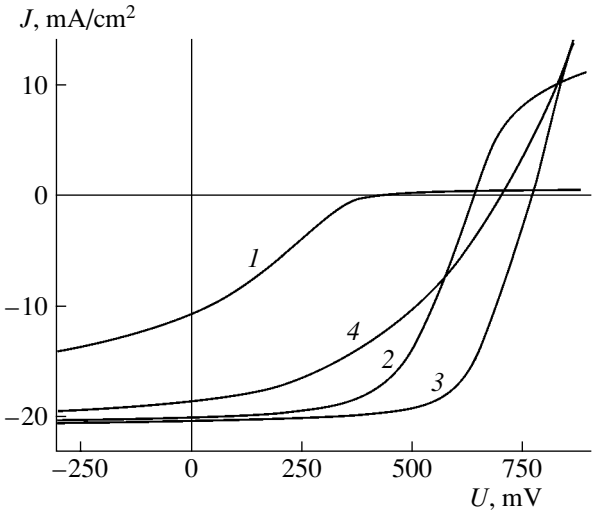

Fig. 1. *I–V* characteristics exhibited under illumination for ITO/CdS/CdTe/Cu/Au solar cells in relation to the thickness of the $CdCl_2$ layer. (*1*) No $CdCl_2$ layer: U_{oc} = 400 mV, J_{sc} = 10.7 mA/cm^2, FF = 0.280, and η = 1.19%; (*2*) the $CdCl_2$ layer is 0.06 μm thick: U_{oc} = 645 mV, J_{sc} = 19.0 mA/cm^2, FF = 0.576, and η = 7.4%; (*3*) the $CdCl_2$ layer is 0.35 μm thick: U_{oc} = 773 mV, J_{sc} = 20.1 mA/cm^2, FF = 0.670, and η = 10.3%; and (*4*) the $CdCl_2$ layer is 1.20 μm thick: U_{oc} = 702 mV, J_{sc} = 19.0 mA/cm^2, FF = 0.414, and η = 5.5%.

3. RESULTS AND DISCUSSION

We measured the *I–V* characteristics exhibited under illumination for the ITO/CdS/CdTe/Cu/Au solar cells obtained using $CdCl_2$ layers of various thicknesses (Fig. 1). Three characteristic intervals can be separately identified in the dependences of the output characteristics and efficiency on the thickness of the $CdCl_2$ layer. An increase in the thickness of the $CdCl_2$ layer up to 0.06 μm leads to an increase in the solar cell efficiency from η = 1.1% to η = 7.4% (Fig. 1, curves *1*, *2*). This increase in the efficiency is equally governed by an increase in all the output parameters. As the thickness of the $CdCl_2$ layer increases from 0.06 to 0.35 μm, the solar cell efficiency increases from η = 7.4% to η = 10.3% due to an increase in the open-circuit voltage and filling factor of the *I–V* characteristic under illumination (Fig. 1, curves *2*, *3*). A further increase in the $CdCl_2$ layer thickness from 0.35 to 1.20 μm leads to a decrease in the solar cell efficiency from 10.3 to 5.4%, which is caused by a decrease in the filling factor of the *I–V* characteristic under illumination (Fig. 1, curves *3*, *4*).

Two diffraction maxima are revealed at the angles 2θ = 23.56° and 2θ = 75.92° in the X-ray diffraction pattern of the ITO/CdS/CdTe heterostructure without the chloride treatment, which was recorded using Bragg–Brentano focusing (Fig. 2a). According to ASTM File no. 15-0770, these reflections can be identified with those from the (111) and (333) planes of cubic CdTe, which indicates that the base layer is textured. The texture axis is the [111] direction, and the degree of texture scattering is 10°. Since we failed to reveal reflection from the CdS layer in the X-ray diffraction pattern of the ITO/CdS/CdTe heterostructure, we also recorded the X-ray diffraction pattern of an ITO/CdS heterostructure. It was found that these CdS films, which belong to a hexagonal crystal system, are textured along the [0002] direction. The application of scanning microscopy to a transverse cleaved surface of the ITO/CdS/CdTe device heterostructure showed that the CdTe and CdS layers are columnar and that the grain size for CdTe is governed by the grain size for CdS. Thus, the emergence of texture in the base layers is governed by oriented growth of CdTe on the textured CdS layers. According to [1], the columnar structure of the base layers provides a substantial decrease in the deleterious effect of the grain-boundary surface on photoelectric processes. However, the ITO/CdS/CdTe/Cu/Au solar cells that were not subjected to the chloride treatment had η of about 1% (Fig. 1, curve *1*).

The data of ASTM File no. 19-0193 show that the reflections revealed by the structural analysis of the ITO/CdS/CdTe heterostructures can also be identified with those from the (002) and (006) planes of metastable hexagonal CdTe. In this case, the texture axis for the base layer is the [0001] direction. In order to resolve the problem of which of the two modifications occurs in the sample under study, we carried out skew recordings. It was found that an attempt to introduce the (105) plane

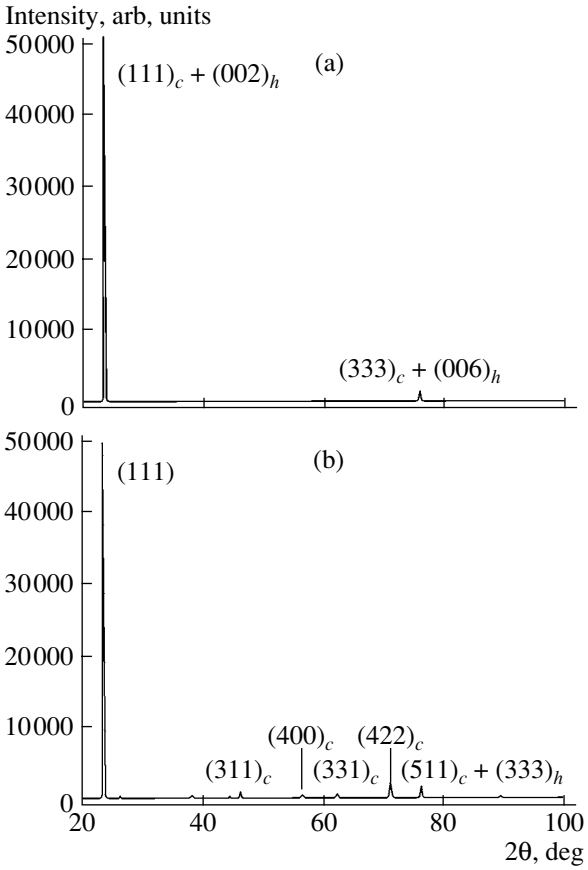

Fig. 2. X-ray diffraction patterns of ITO/CdS/CdTe heterostructures exposed to radiation from a copper anode with Bragg–Brentano focusing (a) prior to the chloride treatment and (b) after the chloride treatment with the use of a $CdCl_2$ layer 0.06 μm thick.

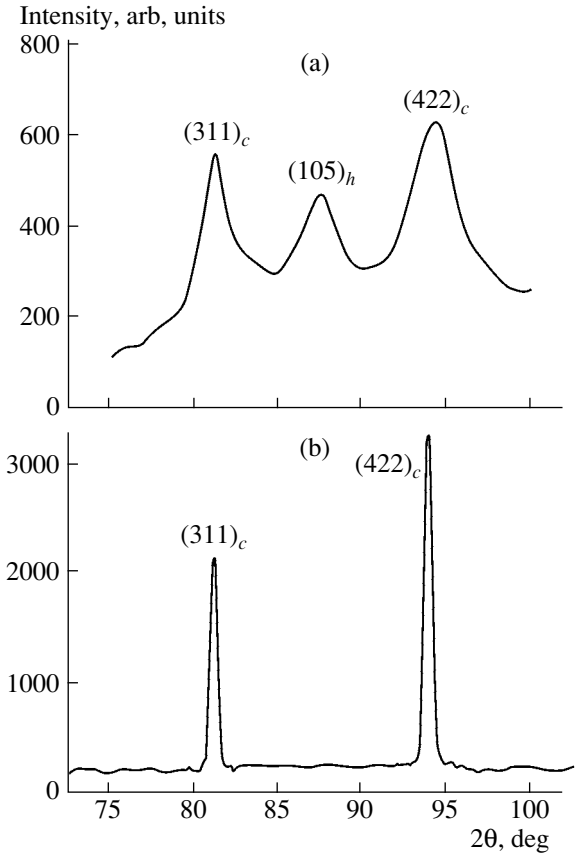

Fig. 3. X-ray diffraction patterns of ITO/CdS/CdTe heterostructures exposed to radiation from an iron anode after sample rotation by 22° (a) prior to the chloride treatment, and (b) after the chloride treatment with the use of a $CdCl_2$ layer 0.06 μm thick.

of the hexagonal modification into the reflecting position also introduces the (331) and (422) planes of the cubic modification into this position (Fig. 3a). This circumstance is associated with the fact that the angles between the (002) and (105) planes of the hexagonal modification and the angles between the (111) and (331) planes and the (111) and (422) planes of the cubic modification differ only slightly. Their magnitudes are 20.7°, 22.0°, and 19.5°, respectively. Thus, in the initial state, the CdTe base layer is two-phase, and the solar cell efficiency is low. A two-phase state, twinning, and a high density of stacking faults are characteristic of CdTe films (see, for example, [9]) because of the insignificant (about 1% [10]) difference between the energies at which the cubic and hexagonal crystal lattices are formed and the low energy at which stacking faults are formed.

Using the method of skew recording, we showed that the chloride treatment of the CdTe films when the thickness of the $CdCl_2$ layer was equal to 0.06 μm leads to the formation of single-phase layers with a stable cubic modification (Fig. 3b). We observed a decrease in the width of the diffraction peaks for reflections from the (331) and (422) planes. This result qualitatively demonstrates that, along with a decrease in microstrain and an increase in the coherent scattering region, the density of stacking faults also decreases. The sensitivity of these lines to stacking faults is associated with the fact that $|h + k + l| = 3N \pm 1$ for them.

The reflections from planes (331), (400), (331), (422), and (511) + (333) of the cubic modification are revealed in the X-ray diffraction pattern, recorded using Bragg–Brentano focusing, of the CdS/CdTe heterostructure with a $CdCl_2$ layer 0.06 μm thick and subjected to chloride treatment (Fig. 2b). This observation indicates that the texturization of the base layer decreases. The degree of texture scattering is 5° (Fig. 3b). The experimentally observed decrease in the degree of texture scattering from 10° to 5°, despite a decrease in the structure quality, is associated with the fact that a texture of only one type is formed in the base CdTe layer after the chloride treatment, specifically, in the [111] direction.

We found that an increase in the thickness of the $CdCl_2$ layer from 0.06 to 0.35 μm leads to an increase

in the degree of texture scattering to 9.3°. The angular width of the (331) and (422) reflections decreases, which suggests a further decrease in the microstrain and density of stacking faults and to an increase in the sizes of the coherent scattering region. We also observed a decrease in the lattice constant of CdTe from $a = 6.494$ Å to $a = 6.488$ Å. According to ASTM File no. 15-0770, the lattice constant of strain-free CdTe layers of high structural quality is 6.481 Å. Therefore, the base CdTe layers subjected to chloride treatment with the use of a $CdCl_2$ layer 0.35 μm thick exhibit less lattice strain than when a $CdCl_2$ layer 0.06 μm thick is used. The experimentally observed lattice constant of the CdTe layer is larger than its theoretical value. This circumstance can be attributed to a difference of 9.7% between the lattice constants of the CdS and CdTe layers [11]. Due to this difference, an oriented CdTe layer grown on a CdS layer is strained. The strain causes an increase in the lattice parameter of the base layer.

According to the phase diagram of the CdTe–$CdCl_2$ system, the Cl atoms possess subatomic solubility in CdTe at the chloride treatment temperatures [12]. Therefore, after the chloride treatment, Cl is experimentally observed on the grain surface of the base layer rather than in the grain bulk [13]. The physical mechanism by which Cl causes structural variations in the CdTe layers relies on the formation of CdO and $TeCl_2$ compounds on the grain-boundary surface of the base layer in the course of annealing in air [14]. Since $TeCl_2$ is a gas under the annealing temperatures used, its presence leads to an increase in mobility of the Cd and Te atoms. This increased mobility leads to nucleation in the spacings between the CdTe grains [15]. It is evident that the nuclei are formed in the intergrain spacings near which the Cl content necessary for the above-mentioned structural transformations of CdTe is required. Therefore, CdTe starts to recrystallize from the surface [16]. This phenomenon causes the experimentally observed decrease in the texturization of the CdTe base layers after the chloride treatment. Since the base layer grows on the CdTe layer during recrystallization, this circumstance causes a decrease in the lattice strain and, correspondingly, lowers the lattice period. Such recrystallization also causes a decrease in the stacking fault and twin density and an increase in the sizes of the coherent scattering region, which leads to the experimentally observed decrease in the width of the diffraction maxima corresponding to the (331) and (422) planes of cubic CdTe (Fig. 3b).

As the thickness of the $CdCl_2$ layer is further increased from 0.35 to 1.20 μm, the lattice constant increases from $a = 6.488$ to 6.494 Å. This increase is accompanied by a decrease in the degree of texture scattering from 9.3° to 8.2°, while the angular width of reflections (331) and (422) increases. It has been shown that the Cl atoms are segregated on the CdS/CdTe interface if the $CdCl_2$ layer is excessively thick [17]. Therefore, nucleation can also start near this interface and not just in the bulk during recrystallization of the base layer in this case. As a result, there is an increase in the orienting effect of CdS on the crystal structure of the CdTe layer. We experimentally revealed the crystal lattice strain of the base layer, which leads to an increase in the lattice constant. The probability of emergence of stacking faults and twins in the base layer also increases. An increase in their concentration in the base layer causes the observed increase in the width of the diffraction peaks that correspond to the (331) and (422) planes of cubic CdTe.

4. CONCLUSIONS

As the thickness of the $CdCl_2$ layer increases to 0.06 μm, transformation of the two-phase CdTe base layer to a single-phase one exerts a determining effect on the intensification of the photoelectric properties of CdS/CdTe thin-film heterostructures. Metastable hexagonal CdTe transforms into a stable cubic phase.

A further increase in the thickness of the $CdCl_2$ layer to 0.35 μm leads to optimization of the photoelectric properties of CdS/CdTe heterostructures due to a decrease in the crystal-lattice strain, a decrease in the stacking fault and twin concentration, and an increase in the sizes of the coherent scattering regions of the base layer. This behavior is caused by the specific features of recrystallization of CdTe during chloride treatment, which leads to a decrease in the orienting effect of the CdS layer on the crystal structure of CdTe.

Excess thickness of the $CdCl_2$ layer (above 0.35 μm) causes a decrease in the efficiency of the photoelectric processes in the CdTe layer. This decrease is caused by the fact that, as the Cl content at the CdS/CdTe interface increases, cubic CdTe can nucleate near the CdTe surface. Due to this circumstance, during rectystallization of the base layer, the orienting effect of CdS on the crystal structure of the base layer is enhanced.

REFERENCES

1. M. A. Green, Prog. Photovoltaics **9**, 123 (2001).
2. X. Wu, J. C. Keane, R. G. Dhere, *et al.*, in *Proceedings of 17th European Photovoltaic Solar Energy Conference* (Munich, Germany, 2001), p. 995.
3. K. Durose, P. R. Edwards, and D. P. Halliday, J. Cryst. Growth **197**, 733 (1999).
4. H. R. Moutinho, F. S. Hasoon, F. Abulfotuh, and L. L. Kazmerski, J. Vac. Sci. Technol. **13**, 2877 (1995).
5. B. E. McCandless, Mater. Res. Soc. Symp. Proc. **668**, H1.6.1 (2001).
6. P. R. Edwards, S. A. Galloway, and K. Durose, Thin Solid Films **372**, 385 (2000).
7. A. Taylor and H. Sinclair, Proc. Phys. Soc. London **57**, 126 (1945).
8. P. A. Panchekha, O. G. Alaverdova, and V. I. Gnidash, Ukr. Fiz. Zh. **45** (1), 75 (2000).
9. P. A. Panchekha, Funct. Mater. **4**, 199 (1997).

10. I. P. Kalinkin, V. V. Alekseevskiĭ, and A. I. Simashkevich, *Epitaxial Films of the II–VI Compounds* (Leningr. Gos. Univ., Leningrad, 1978), p. 54 [in Russian].
11. R. H. Bube, *Properties of Semiconductor Materials: Photovoltaic Materials* (Imperial College Press, USA, 1999), Vol. 1, p. 136.
12. G. S. Oleinik, P. A. Mizetskii, and T. P. Nuzhnaya, Inorg. Mater. **22**, 164 (1986).
13. M. Terheggen, H. Heinrich, G. Kostorz, *et al.*, in *Proceedings of EMRS Spring Meeting* (Strasburg, France, 2002), B-X4.
14. B. E. McCandless, Mater. Res. Soc. (Warrendale, PA, 2001), H1.6.1.
15. H. R. Moutinho, M. M. Al-Jassim, F. A. Abulfotuh, *et al.*, in *Proceedings of 6th IEEE Photovoltaic Specialist Conference* (Anaheim, USA, 1997), p. 431.
16. A. Romeo, A. N. Tiwari, and H. Zogg, in *Proceedings of 2nd World Conference and Exhibition on Photovoltaic Solar Energy Conversion* (Vienna, 1997), p. 1105.
17. M. Terheggen, H. Heinrich, G. Kostorz, *et al.*, in *Proceedings of 17th European Photovoltaic Solar Energy Conference* (Munich, Germany, 2001), p. 1188.

Translated by N. Korovin